Selective neutron transmutation doping with Gd masks in GaN semiconductors

Jeongwoo Kim[a], Matthias Frontzek[b], Lowell Crow[b], and Jae Kwon[a]
[a]*Department of Electrical Engineering and Computer Science, University of Missouri, Columbia, Missouri 65211*
[b]*Neutron Sciences Directorate, ORNL, Oak Ridge, Tennessee 37831, USA*

Abstract

For the first time, selective neutron transmutation doping was successfully performed on GaN through Gd masks, showing the feasibility of patternable doping through neutron irradiations. In collaborating with Oak Ridge National Laboratory, GaN with Gd masks was irradiated by directional neutrons. By using the Gd properties with high neutron absorption cross-sections, it was confirmed that the area covered by Gd masks on GaN was completely shielded from neutron, and the uncovered area was doped with the generated Ge and ^{14}C. The difference was clearly identified in various ways when comparing the area exposed by neutrons and the area unexposed by neutrons. The discoloration by the ejected protons and elastic scattering of neutrons appeared only in the exposed area, and the unexposed area was the same as before irradiation. The neutron scattering angle in GaN was estimated by comparing the front and backside. From energy dispersive x-ray spectroscopy spectra and secondary ion mass spectrometry measurement, the concentration difference as well as the exact concentration of produced ^{14}C was also checked. Schottky barrier diodes on the selectively doped GaN were fabricated and investigated to study the electrical properties.

Keywords

GaN, Neutron transmutation doping, Selective doping, neutron shielding by Gd

1. Introduction

Gallium nitride (GaN) is considered a promising semiconductor material for the next generation due to its large wide bandgap (3.4 eV), which makes GaN have superior electrical conductivity, breakdown properties, and switching speed [1-10]. Especially, such properties are highly desired for various power electronic devices. Development of controlling doping in a reliable way is of great importance for the high performance GaN-based power devices. GaN doping is possible in two forms – doping during wafer growth and post-growth doping.

Epitaxial techniques are widely used as one of the doping method during wafer growth and basically consists three different types: metalorganic chemical vapor deposition (MOCVD), hydride vapor phase epitaxy (HVPE), and molecular beam epitaxy (MBE). The MOCVD and HVPE are based on chemical deposition method and obtain the doping by introducing gases containing certain amount of dopant into the reactor. The MBE is a vacuum technique. In high-vacuum chambers, dopants come from high purity solid sources as an evaporated form and are incorporated into GaN substrate.

According to growth speed or wafer quality, the epitaxial techniques above are utilized. However, it is still hard to get epilayers with low doping concentration and necessarily requires additional procedures like lithography, etching, and regrowth. As a more commonly applied for selective doping, the ion implantation technique is the other doping method during wafer growth. It is less demanding and easy to control the all ranges of concentrations while the process has a very big disadvantage of destroying the crystal structure of the material. In order to rebuild it, it is required high temperature (normally > 1100 ℃) heat treatment. Sometimes, the process is performed at more than 1400 ℃, resulting in serious surface decomposition [11,12]. Different from the approaches described above, the selective neutron transmutation doping (NTD) process can be another method for doping.

The NTD process does not need the additional procedures and high temperature heat treatment. Furthermore, the advantages of this novel approach include repeated doping in the same material if annealing or radiation damage is acceptable, post-growth doping, and homogeneity of doping [13,14]. The most interesting advantage of the NTD process is to obatin extremely consistent and uniform doping, which was confirmed in GaN wafer as well as Si wafer [15]. Although a nuclear reactor with necessary irradiation conditions is required, various research reactors worldwide can be and have been performing the NTD process.

In GaN, three major reactions are triggered by neutrons during the NTD process: $^{69}Ga(n,\gamma)^{70}Ge$, $^{71}Ga(n,\gamma)^{72}Ge$, and $^{14}N(n,p)^{14}C$. Gallium (Ga) initially produces unstable Ga through a (n,γ) reaction and follows the β^- decay to become stable isotopes of germanium (Ge). Nitrogen (N) undergoes a (n,p) reaction and produce carbon-14 (^{14}C). These three reactions can be expressed as the following formulas: (X* means that element X is unstable)

$$^{69}_{31}Ga \ + \ ^{1}_{0}n \rightarrow \ ^{70}_{31}Ga^{*} \rightarrow \ ^{70}_{32}Ge \ + \ ^{0}_{-1}\beta \ ;$$

$$^{71}_{31}Ga \ + \ ^{1}_{0}n \rightarrow \ ^{72}_{31}Ga^{*} \rightarrow \ ^{72}_{32}Ge \ + \ ^{0}_{-1}\beta \ ;$$

$$^{14}_{7}N \ + \ ^{1}_{0}n \rightarrow \ ^{14}_{6}C^{*} \ + \ ^{1}_{1}p \ ;$$

As a favorable n-type dopant in GaN, Ge has been widely used recently instead of silicon (Si). One of the advantages of Ge as an n-type dopant is that Ge substituting on the Ga site induces far less stress as the atom radius of Ge is similar to Ga [16-18]. With the benefit, Ge produced during the NTD process is an even homogeneity dopant and dopes GaN as an n-type.

In reactor physics, neutrons are roughly parameterized into three groups based on their energy; thermal neutrons have less than 1 eV, epithermal neutrons have between 1 eV and 100 keV, and fast neutrons have great than 100 keV. In the energy range with the thermal and epithermal neutrons, the three reactions mentioned above have high cross-sections, as shown in Figure 1. a. Oppositely, gadolinium (Gd) isotopes have very high neutron absorption cross-sections in Figure 1. b

and have been commonly utilized as neutron absorber [19,20]. Utilizing the neutron shielding of Gd, GaN can be selectively doped by Ge produced during the NTD process if GaN is covered with Gd masks with patterns.

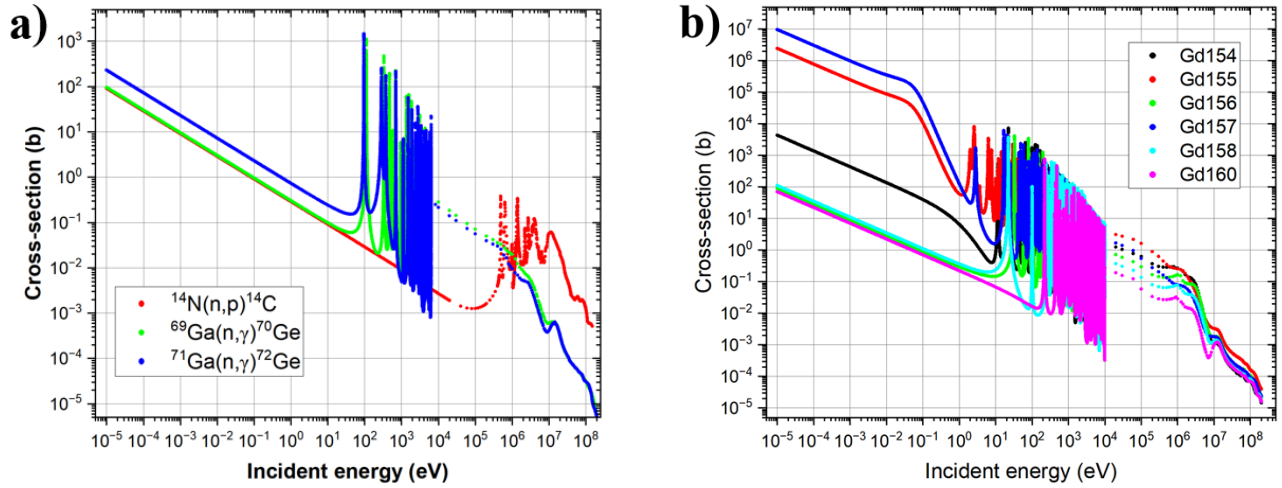

Figure 1. a) cross-sections for major reactions in GaN during the NTD: ^{69}Ga(n,γ)^{70}Ge, ^{71}Ga(n,γ)^{72}Ge, and ^{14}N(n,p)^{14}C. b) neutron absorption cross-sections of stable Gd isotopes: ^{154}Gd, ^{155}Gd, ^{156}Gd, ^{157}Gd, ^{158}Gd, and ^{160}Gd.

In this article, selectively doped GaN samples are developed by directional neutron irradiations in Oak Ridge National Laboratory (ORNL) to investigate the optical, atomic and, electrical characteristics and compare the properties of GaN with or without Gd masks. The optical properties of the GaN are studied from optical images and scanning electron microscopy (SEM) images. Through secondary ion mass spectrometry (SIMS) measurements and energy dispersive x-ray spectroscopy (EDS) spectra, atoms generated during the irradiation are quantified. After fabricating Schottky barrier diodes (SBDs), the electrical properties are compared by using current-voltage (I-V) characteristics, Cheung's functions, and capacitance-voltage (C-V) characteristics.

2. Materials and methods

2.1. Appropriate thickness of Gd mask for neutron shielding

The attenuation of neutron dose by Gadolinium (Gd) shadow mask is calculated by the following equation:

$$\frac{I(t_x)}{I_0} = e^{-N \cdot t_x \cdot \sigma}$$

where $I(t_x)$ is the neutron flux when it penetrates the t_x thickness of the Gd mask, I_0 is the initial neutron flux without any attenuation. N is the atomic number density of natural Gd (3.025×10^{23} atoms/cm^3), t_x is the thickness of Gd shadow mask, and σ is the neutron reaction cross section for natural Gd (49,300 barn). $I(t_x)/I_0$ is the transmission rate of neutron dose depending on the thickness of a Gd mask.

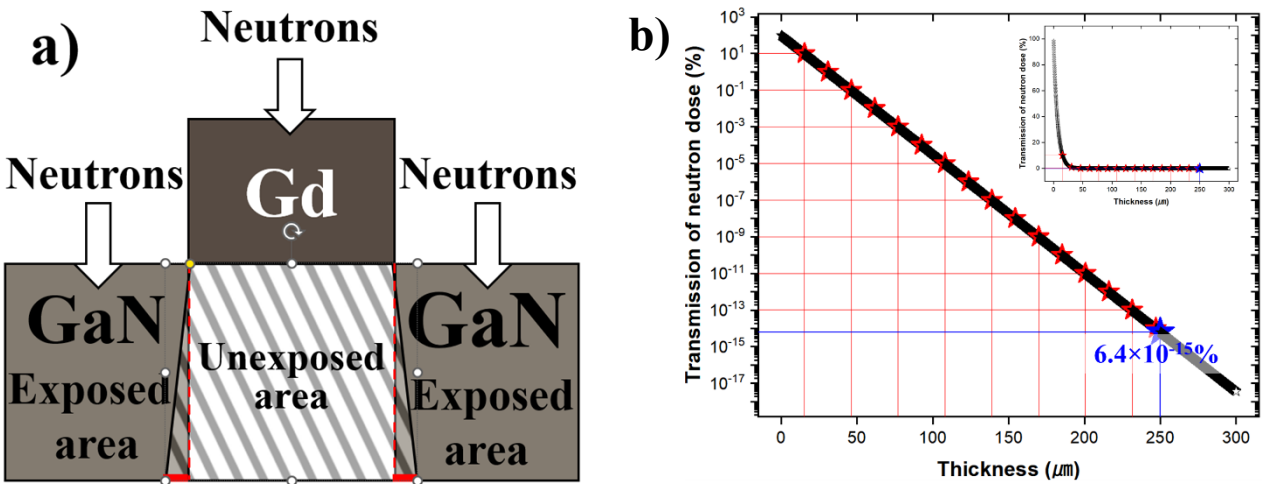

Figure 2. a) Diagram of GaN with a Gd mask and b) the transmission rate of neutron dose depending on the Gd thickness.

Figure 3 shows the diagram of Gd shadow mask on GaN and the transmission rate of neutron dose. Over 123 μm thickness, Gd masks can make a 10^5-fold neutron dose difference. 250 μm thickness of Gd masks were used for more clear shielding. There were two Gd masks with different patterns; one was a rectangular pattern and the other was a circular pattern. Two square (1 cm^2) GaN samples were from Adroit Materials.

2.2. Irradiations [**Please check this part**]

In collaboration with ORNL, the GaN samples were irradiated using the HB-2D instrument at the High Flux Isotope Reactor (HFIR). HB-2D is a test and development beamline located at the HB-2 beamtube which is radially from the reactor core. The neutron beam of HB-2 is filtered through a sapphire crystal array, cooled by liquid nitrogen which results in transmission of less than 10 % for neutrons with energy higher than 500meV [ref J. Appl. Cryst. (1993). 26, 438-447] in the HFIR HB-2 neutron spectrum. The straight neutron beam from the HB-2 beam tube is normally monochromated and reflected by a single crystal array to perform neutron scattering experiments. Here, the straight neutron beam was usedto perform directional neutron irradiation with the full thermal spectrum. For this purpose, GaN samples were first wrapped in aluminum (Al) foil with Gd masks were mounted on an aluminum sheet using aluminum wire. The sheet was screwed with aluminum screws to a mounting plate. The mounting plate has a hanger which fits over the rim of the HB-2D collimator insert. A threaded hole on top of the adaptor could be connected to a long pole with a threaded tip to reliably lower and retrieve the mounting plate with good reproducibility. Figure 3. a. shows a view from the top into the HB-2D monochromator shielding with the mounting plate and sample in place for an irradiation.

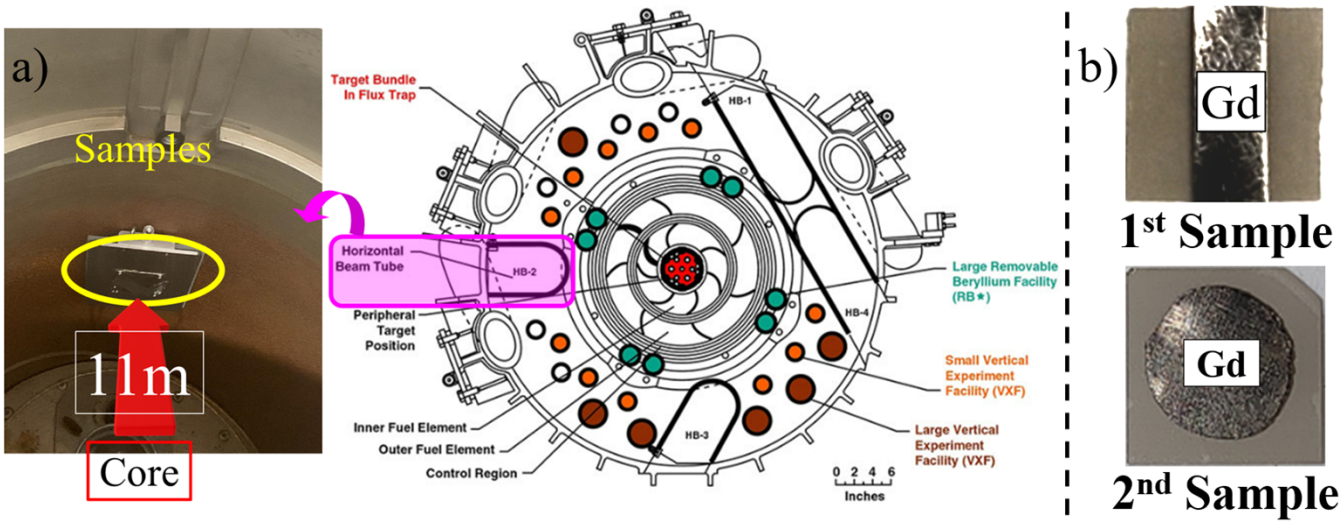

Figure 3. Appearance of a) the HB-2D port where the sample is mounted, 11m from the core in HFIR of ORNL; a schematic shows the HB-2 beam tube orientation within the 1.1 m diameter HFIR core and b) GaN samples with Gd masks.

The distance is 11 m between the core and the sample holder. From the neutron activation of Ga an average thermal neutron flux of 5.5×10^9 neutrons/cm^2/s was calculated for this position. One cycle at HFIR is on average 24 days long. For the 1st irradiation, one GaN sample with the rectangular pattern was irradiated for one cycle. Initial analysis showed that longer irradiation times were necessary and therefore the second set of samples was irradiated for 3 cycles at the 2nd irradiation.

[Details of irradiation process and some images]

2.3. Annealing and SBD fabrication

The ejected proton generated during the $^{14}N(n,p)^{14}C$ reaction and elastic scattering of neutrons dislocating Ga and N atoms can cause damage to the GaN lattice and result in a discoloration of GaN. The samples with such damages have no or poor optical and electrical characteristics. The annealing process can reverse the damages and was performed on GaN samples for 10 minutes at 935 °C with NH_3 ambient. SBDs were fabricated to measure the electrical characteristics. Pt/Au (80 nm / 40 nm) were deposited on the polished side of GaN for Schottky contact, and Ti/Au (30 nm / 150 nm) were deposited on the unpolished side of GaN for Ohmic contact. The GaN samples with metal layers were rapidly annealed for 1 minute at 650 °C with N_2 ambient to improve the metal contact

2.4. Electrical parameters calculated by I-V characteristics, Cheung's functions, Norde function, and C-V characteristics

The current through the SBDs at a forward bias ($V \geq 3kT/q$) follows the thermionic emission theory [21] and can be expressed as:

$$\boldsymbol{I} = I_0 e^{\frac{qV}{\boldsymbol{n}kT}}$$

$$\boldsymbol{I_0} = AA^{**}T^2 e^{-\frac{q}{kT}\boldsymbol{\Phi_b}}$$

where, A is the diode area (5.027×10^{-3} cm^{-2}), A** is the effective Richardson constant (35 $A/(cm^2\cdot K^2)$ [22], T is the absolute room temperature (300 K), q is the charge of an electron (1.6×10^{-19} C), k is the Boltzmann's constant (1.381 × 10-23 J/K), ϕ_b is the measured barrier height, and n is the ideality factor. The ϕ_b and n are calculated using the reverse leakage current at -1 V. Shunt resistance (R_{Sh}) is estimated from the junction resistance obtained by $R_j = \frac{\partial V}{\partial i}$ from the I–V characteristics.

Cheung's method was used to determine the ϕ_b, n, and R_S of the SBDs in the non-linear forward-bias region of the lnI-V curve [23]. According to Cheung's functions, each value can be estimated from the following equations:

$$\frac{\boldsymbol{d(V)}}{\boldsymbol{d(lnI)}} = \frac{kT}{q} \times \boldsymbol{n} + \boldsymbol{R_S} \times I$$

$$\boldsymbol{H(I)} = V - \frac{nkT}{q} ln\left(\frac{I}{AA^{**}T^2}\right) = I \times \boldsymbol{R_S} + n \times \boldsymbol{\Phi_b}$$

The forward-bias dV/d(lnI) versus I and H(I) versus I show linear behavior. The slope and y-axis intercept of dV/d(lnI) versus I curve give R_S and n. Using the ideality factor value calculated from dV/d(lnI) versus I curve, ϕ_b, n, and R_S are obtained from the slope and y-axis intercept of the H(I) versus I curve.

The C-V characteristics of the SBDs were measured at a frequency of 1 MHz. ϕ_b and carrier concentration (CCC) is determined from plots of $1/C^2$-V characteristics based on the following equations [24]:

$$\boldsymbol{\phi_b = V_{bi} + V_P}$$

$$\frac{\boldsymbol{1}}{\boldsymbol{C^2}} = \frac{2(\boldsymbol{V_{bi}} - \frac{kT}{q} - V)}{A^2 \times q \times N \times \varepsilon_s}$$

$$\boldsymbol{V_P} = \frac{kT}{q} ln(\frac{N_C}{N})$$

where V_{bi} is the built-in potential ($V_{bi} = V_0 + \frac{kT}{q}$), N is the carrier concentration, ε_S is the dielectric constant of GaN (8.9 ε_0 = 7.88×10^{-11} F/m), N_C is the effective conduction band density of states in GaN (2.3×10^{18} cm^{-3}). V_0 is determined by the x-intercept of the $1/C^2$ versus V curve.

3. Results and discussion

3.1. Optical characteristics

As the irradiation time increased, the border line became clearer due to damages induced by neutron irradiations. In Figure 4, the unexposed areas shielded by Gd masks are brighter than the exposed areas and even very similar to GaN before irradiation. Cutting out Gd with high precision is very difficult, resulting in bending at the edge. Considering that, the neutron scattering angle is approximately 5 degree.

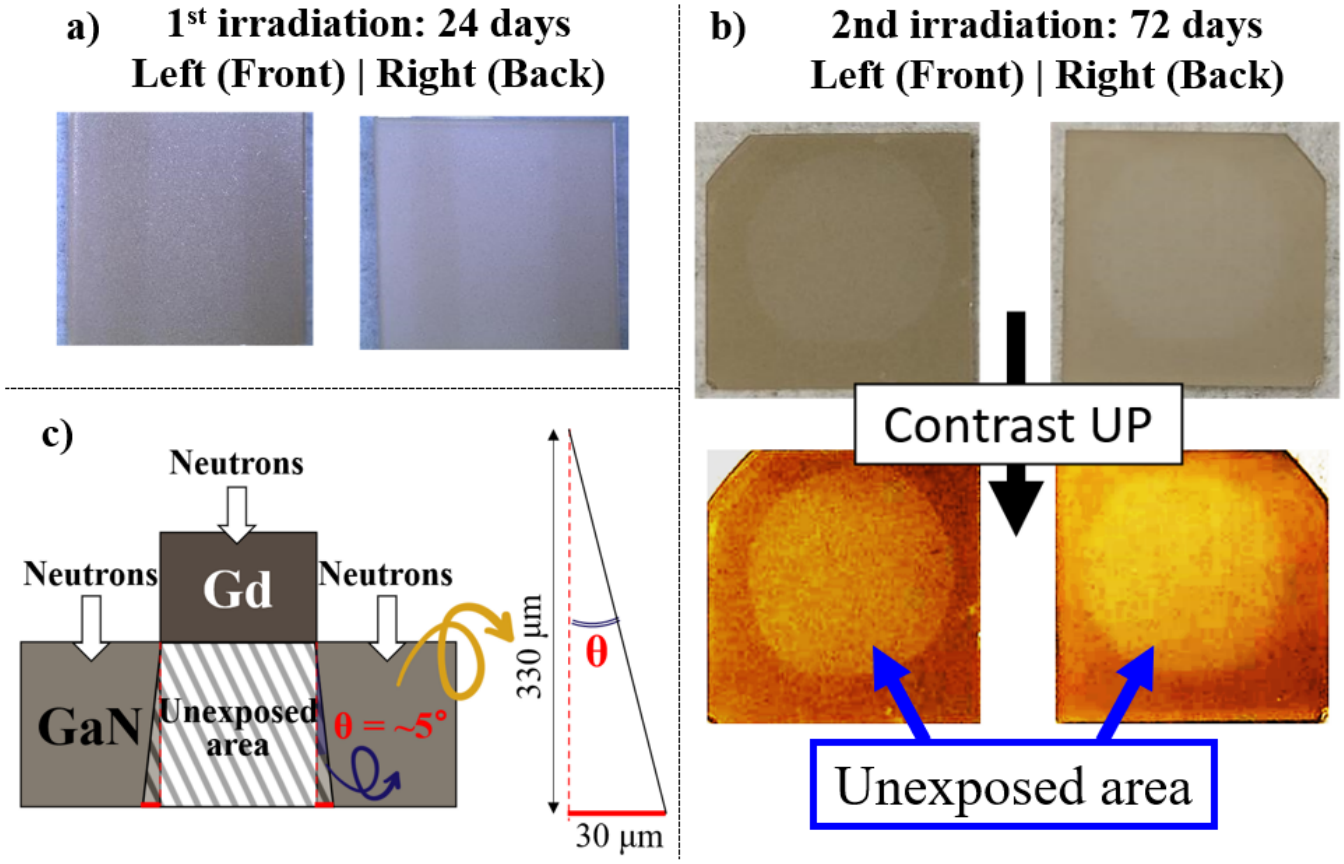

Figure 4. a) optical images of 1st irradiation sample, b) optical images of 2nd irradiation sample, and c) measurement for neutron scattering angle in GaN

The difference between the exposed area and the unexposed area was confirmed by SEM images, as shown in Figure 5. a. In the exposed area, some black patterns in Secondary Electron (SE) detector images were detected while the black patterns are very blurry in Backscatter Electron (BSE) detector image. The clear patterns in the SE image mean something on the surface changes the topography of GaN's surface. Sometimes, that kind of pattern is confused with a physical scratch or organic matter. The BSE images confirmed that the black patterns were not scratch or organic matter and even showed that the black patterns have very similar chemical properties to the unexposed GaN and look similar to graphene [25].

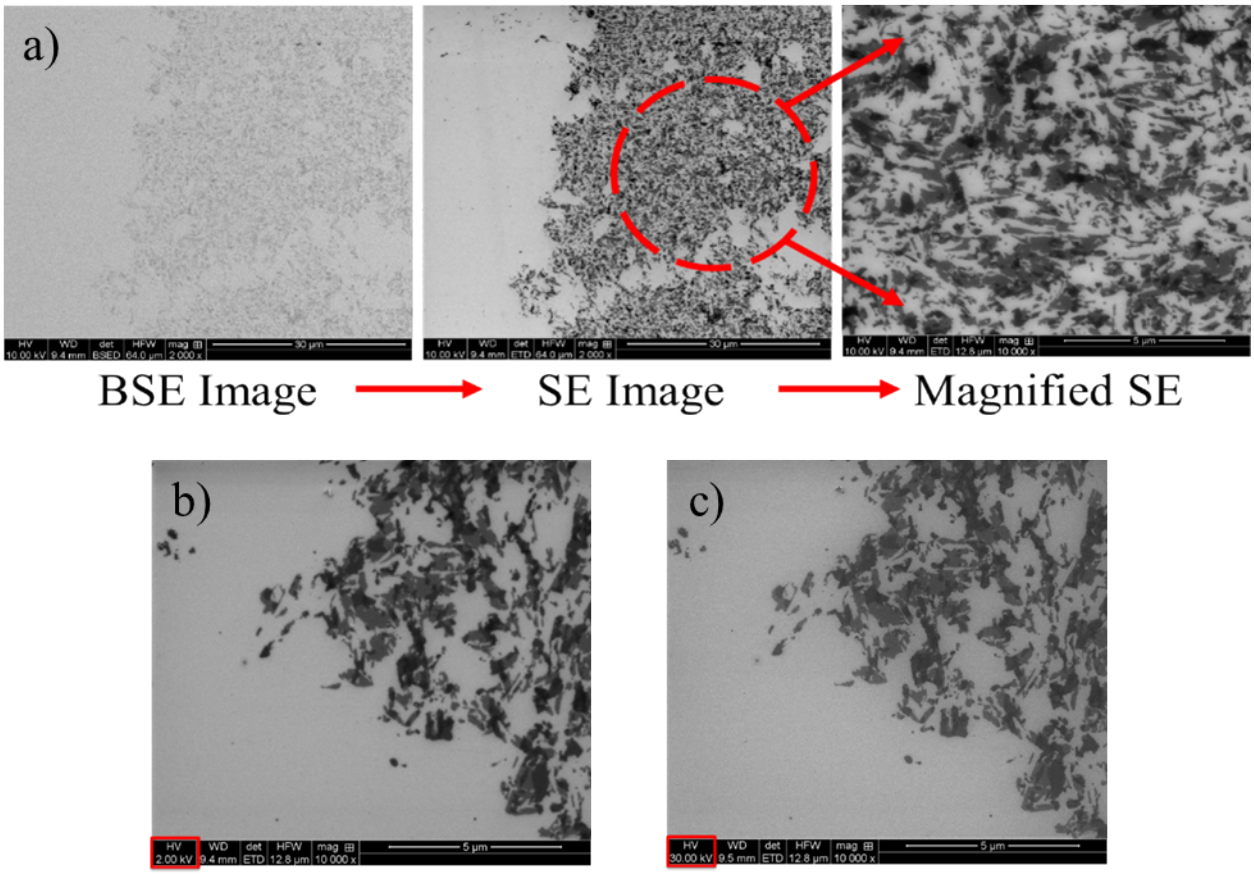

Figure 5. a) SEM images near the borderline between the exposed and unexposed area, b) SE image measured by 2 kV, and c) SE image measured by 30 kV.

Interestingly, the pattern is not only on the surface. Based on the mechanism of the SEM technique, high voltage measurement can detect deeper parts of an object. If one object is just a tiny particle or shallow layer, it will look more transparent with high voltage than low voltage. However, Figure 5. b is almost the same as Figure 5. c although Figure 5. c was measured at a much high voltage. That means the black patterns are not just particles but uniformly deposited layers. It is believed that the pattern was generated after the NTD process and may a be by-product related to ^{14}C or neutron defects.

3.2. Quantification of by-products

To confirm if the NTD process actually occurred in GaN and produced by-product, the difference in carbon concentration was checked through EDS, as shown in Figure 6. a. The GaN samples already have some carbons included for wafer growth. For the exact comparison, the doping concentration of ^{14}C was measured through SIMS. In the unexposed area, the ^{14}C concentration was below the detection limit and was not detected. Some amount of ^{14}C was measured in the exposed area, which has proven that the NTP process was selectively performed, and neutrons barely penetrated the Gd

mask. The GaN samples were intially doped a lot by Ge (~10^{18}/cm^3) during the growth, making it impossible to measure the produced Ge through SIMS measurements. Based on the ^{14}C doping concentration, it was expected that10^{15} ~ 10^{16}/cm^3 of Ge.

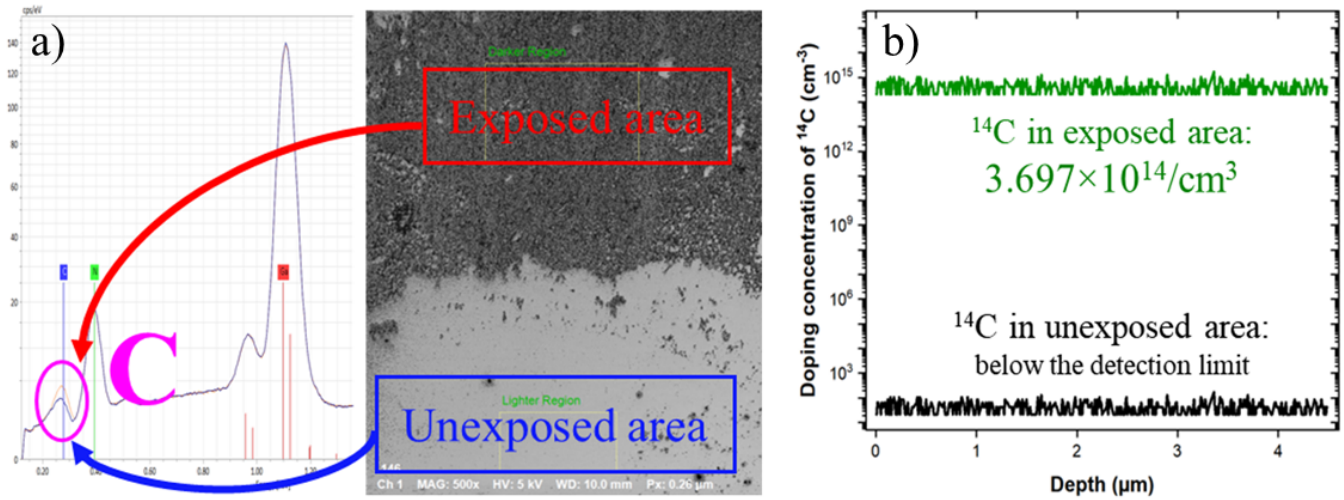

Figure 6. a) EDS spectra in the exposed and unexposed area. The red box is an exposed area, and the blue box is an unexposed area. b) SIMS profile for ^{14}C doping concentration in the exposed and unexposed area.

3.3. Electrical characteristics

Electrical characteristics can be investigated with various electrical parameters – Φ_b, n, R_S, and R_{SH}. Among them, Φ_b and n are key indicators for evaluating the performance of SBDs. According to the methods mentioned at 2.4., the diverse curves were plotted in Figure 7. Based on the curves, electrical parameters were calculated and tabulated in Table I. As expected, it was difficult to see the clear difference in electrical characteristics due to the n-type properties of GaN highly doped during the growth. Overall, SBD fabricated in the exposed area has slightly better Φ_b and n. The resistances are very similar to each other. Some defects, including ^{14}C, were produced, but the amount was negligible and did not affect the electrical properties. The produced Ge improved n-type properties and had more influence on the electrical characteristics. The enhanced quality of n-type semiconductors was more clearly shown in CCC-V and Φ_b-V curves. The SBD in the unexposed area started breakdown earlier than in the exposed area, which was shown in longer CCC curves and higher Φ_b curves.

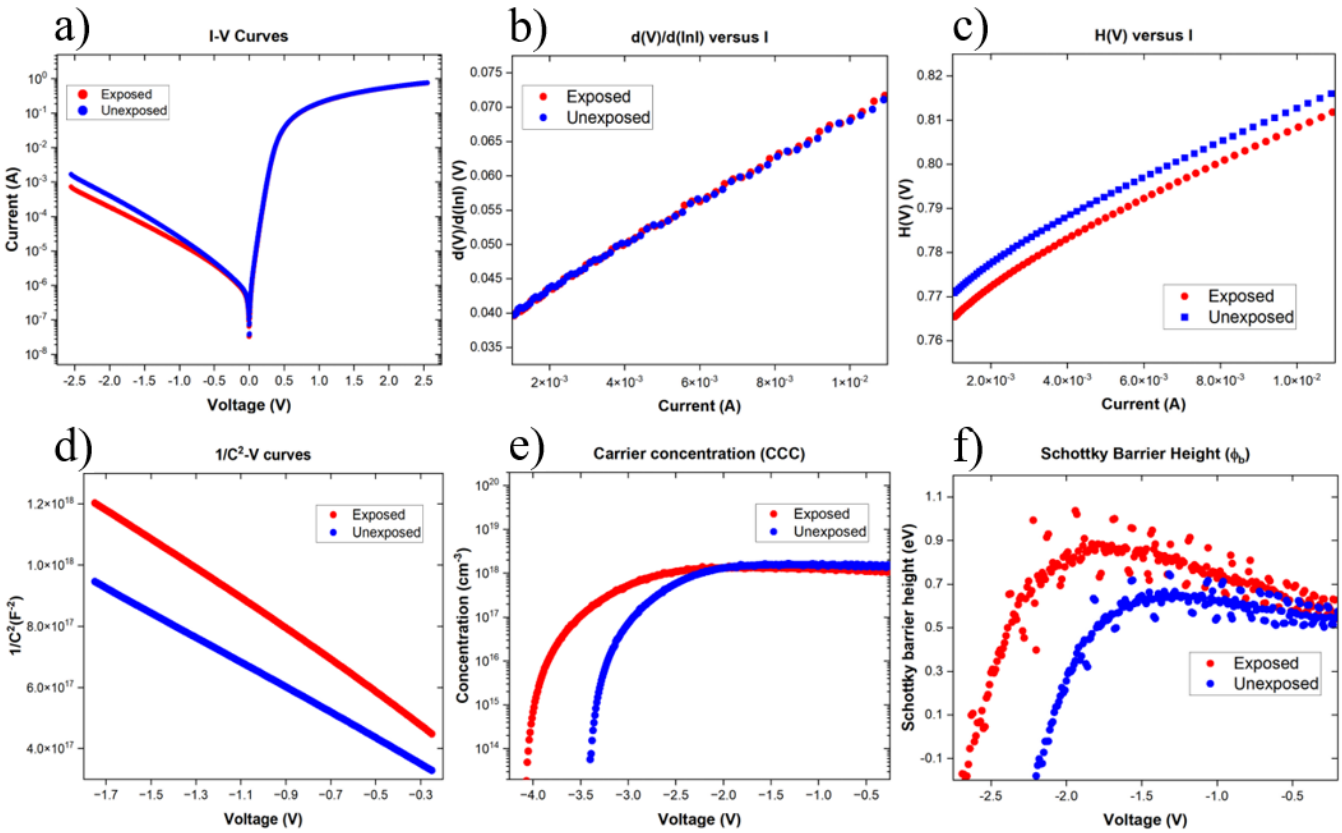

Figure 7. a) I-V curves, b) $\frac{d(V)}{d(lnI)}$-I curves, c) H(V)-I curves, d) 1/C^2-V curves, e) CCC-V curves, and f) Φ_b-V curves of the SBDs in the exposed and unexposed area.

Table 1. The calculated barrier height (Φ_b), ideality factor (n), series resistance (R_S) and shunt resistance (R_{SH}) of the GaN SBDs obtained by I–V characteristics, Cheung's functions, and C-V characteristics.

Method		**Parameters**	**SBD in the unexposed area**	**SBD in the exposed area**
From I-V characteristics		Saturation current at -1V	2.507×10^{-5}	1.675×10^{-5}
		Barrier height Φ_b	0.524 eV	0.534 eV
		Ideality factor n	1.261	1.245
		Shunt resistance R_{Sh}	$2.17\times10^5\ \Omega$	$3.30\times10^5\ \Omega$
From Cheung's functions	$\frac{dV}{d(lnI)}$ versus I	Ideality factor n	1.205	1.189
		Series Resistance R_S	55 Ω	57 Ω
	H(V) versus I	Barrier height Φ_b	0.625 eV	0.629 Ω
		Series Resistance R_S	55 Ω	57 Ω
From C-V characteristics		Barrier height Φ_b	0.582 eV	0.852 eV

4. Conclusions

It was successfully demonstrated that the neutron transmutation doping process could be performed in the selective area depending on the patter of Gd masks. The Gd masks with 250 μm of thickness excellently shielded neutrons and made no transmutation reactions on the unexposed area in GaN. In the exposed area, there were some changes in the optical and electrical characteristics. Damages caused by neutron irradiation created black patterns, which were checked by the discoloration in the optical images. The 5 degrees of neutron scattering angle was measured by comparing the front and backside. Through EDS spectra and SIMS measurement, ^{14}C was measured in the exposed area , not the unexposed area. The Schottky barrier diodes fabricated in the areas weakly showed different n-type properties.

Declaration of interests

The authors declare that they have no known competing financial interests or personal relationships that could have appeared to influence the work reported in this paper.

Acknowledgments

This work has been supported by the ARPA-E project # DE-AR0000874 under the PNDIODES Program, Dr. Isik C. Kizilyalli, Program Director, and Dr. Eric P. Carlson, Technical Support.

References

[1] T. Oka, Recent development of vertical GaN power devices. Jpn. J. Appl. Phys. 58 (2019) SB0805, https://doi.org/10.7567/1347-4065/ab02e7.

[2] H. Amano et al., The 2018 GaN power electronics roadmap. J. Phys. D: Appl. Phys. 51 (2018) 16300, https://doi.org/10.1088/1361-6463/aaaf9d.

[3] J. Hu et al., Materials and processing issues in vertical GaN power electronics. Mat. Sci. Semicond. Process. 78 (2018) 75–84, https://doi.org/10.1016/j.mssp.2017.09.033.

[4] A.V. Inyushkin, A.N. Taldenkov, D.A. Chernodubov et al., High Thermal Conductivity of Bulk GaN Single Crystal: An Accurate Experimental Determination. Jetp Lett. 112 (2020) 106–111, https://doi.org/10.1134/S0021364020140039.

[5] Qiye Zheng, Chunhua Li, Akash Rai, Jacob H. Leach, David A. Broido, and David G. Cahill, Phys. Rev. Materials 3 (2019) 014601, https://doi.org/10.1103/PhysRevMaterials.3.014601.

[6] H. Ohta, N. Asai, F. Horikiri, Y. Narita, T. Yoshida and T. Mishima, Two-Step Mesa Structure GaN p-n Diodes With Low ON-Resistance, High Breakdown Voltage, and Excellent Avalanche Capabilities, in IEEE Electron Device Letters, vol. 41 (2020) pp. 123-126, https://doi.org/10.1109/LED.2019.2955720.

[7] T. Maeda et al., Parallel-Plane Breakdown Fields of 2.8-3.5 MV/cm in GaN-on-GaN p-n Junction Diodes with Double-Side-Depleted Shallow Bevel Termination, 2018 IEEE International Electron Devices Meeting (2018) pp. 30.1.1-30.1.4, https://doi.org/10.1109/IEDM.2018.8614669.

[8] D. Li, C. Ma, J. Wang, F. Hu, Y. Hou, S. Wang, J. Hu, S. Yi, Y. Ma, J. Shi et al., High-Speed GaN-Based Superluminescent Diode for 4.57 Gbps Visible Light Communication. Crystals 12 (2022) 191, https://doi.org/10.3390/cryst12020191.

[9] J. -s. Moon et al., Novel High-speed Linear GaN Technology with High Efficiency, 2019 IEEE MTT-S International Microwave Symposium (2019) pp. 1130-1132, https://doi.org/10.1109/MWSYM.2019.8700832.

[10] Y. Wu, X. Mao, C. Min, D. Yan and H. Chen, GaN FET Push–Pull Driver Circuit Enabling Power Light Emitting Diode to be a High-Efficiency, High-Speed Wireless Transmitter, in IEEE Photonics Journal 10 (2018) pp. 1-10, https://doi.org/10.1109/JPHOT.2018.2879322.

[11] A. Uedono, R. Tanaka, S. Takashima et al., Dopant activation process in Mg-implanted GaN studied by monoenergetic positron beam. Sci Rep 11 (2021) 20660, https://doi.org/10.1038/s41598-021-00102-2.

[12] K. Sierakowski, R. Jakiela, B. Lucznik, P. Kwiatkowski, M. Iwinska, M. Turek, H. Sakurai, T. Kachi, M. Bockowski, High Pressure Processing of Ion Implanted GaN. Electronics 9 (2020) 1380, https://doi.org/10.3390/electronics9091380.

[13] N. M. A. Mohamed, M. Osman, and I. Abdelrazek, Efficient Neutron Irradiation Procedure for Uniform Dopant Distributions in Silicon Doping. ASME J of Nuclear Rad Sci. 8 (2022) 034503, https://doi.org/10.1115/1.4054005.

[14] H. Q. Ho, Y. Honda, S. Hamamoto, T. Ishii, S. Takada, N. Fujimoto, and E. Ishitsuka, Promising Neutron Irradiation Applications at the High Temperature Engineering Test Reactor. ASME J of Nuclear Rad Sci. 6 (2020) 021902, https://doi.org/10.1115/1.4044529.

[15] R. Barber, Q. Nguyen, J. Brockman, et al., Thermal neutron transmutation doping of GaN semiconductors. Sci Rep 10 (2020) 16295, https://doi.org/10.1038/s41598-020-72862-2.

[16] D. Schiavon, E. Litwin-Staszewska, R. Jakieła, S. Grzanka, P. Perlin, Effects of MOVPE Growth Conditions on GaN Layers Doped with Germanium. Materials 14 (2021) 354, https://doi.org/10.3390/ma14020354.

[17] M. N. Fireman, G. L'Heureux, F. Wu, T. Mates, E. C. Young, J. S. Speck, High germanium doping of GaN films by ammonia molecular beam epitaxy, Journal of Crystal Growth 508 (2019) 19-23, https://doi.org/10.1016/j.jcrysgro.2018.12.009.

[18] M. Deppe, J. W. Gerlach, S. Shvarkov, D. Rogalla, H.-W. Becker, D. Reuter, and D. J. As , Germanium doping of cubic GaN grown by molecular beam epitaxy" Journal of Applied Physics 125 (2019) 095703, https://doi.org/10.1063/1.5066095.

[19] Tomasz Piotrowski, Neutron shielding evaluation of concretes and mortars: A review, Construction and Building Materials 277 (2021) 122238, https://doi.org/10.1016/j.conbuildmat.2020.122238.

[20] J. -C. Sublet, A. Koning, D. Rochman, M. Gilbert, A. C. Kahler, C. Jouanne, J. Leppänen, S. v. d. Marck, and P. Romano, Multifaceted coded nuclear data libraries assemblage, verification and validation: TENDL-2019, Transactions of the American Nuclear Society 123 (2020) 1227-1230, https://doi.org/10.13182/T123-33321.

[21] E.H. Rhoderick and R.H. Williams, Metal-Semiconductor Contacts (Clarendon: Oxford, 1988), p. 121.

[22] Kumar, A., Arafin, S., Amann, M.C. et al. Temperature dependence of electrical characteristics of Pt/GaN Schottky diode fabricated by UHV e-beam evaporation. Nanoscale Res Lett 8, 481 (2013), https://doi.org/10.1186/1556-276X-8-481.

[23] S.K. Cheung and N.W. Cheung, Extraction of Schottky diode parameters from forward current-voltage characteristics, Appl. Phys. Lett. 49 (1986) 85, https://doi.org/10.1063/1.97359.

[24] H. Norde, A modified forward I-V plot for Schottky diodes with high series resistance, J. Appl. Phys. 50 (1979) 5052, https://doi.org/10.1063/1.325607.

[25] R.T. Tung, Electron transport at metal-semiconductor interfaces: General theory, Phys. Rev. B 45 (1992) 13509, https://doi.org/10.1103/PhysRevB.45.13509.